Probing the equation of state in the AGS energy range with 3-d hydrodynamics

N. Arbex[1]*, U.Ornik[2]†, M. Plümer[1]‡and R.M. Weiner[1]§

[1] Physics Department, Univ. of Marburg, Marburg, Germany

[2] Soultek Internet Service, Marburg, Germany

Abstract

The effect of (i) the phase transition between a quark gluon plasma (QGP) and a hadron gas and (ii) the number of resonance degrees of freedom in the hadronic phase on the single inclusive distributions of 16 different types of produced hadrons for $Au + Au$ collisions at AGS energies is studied. We have used an exact numerical solution of the relativistic hydrodynamical equations *without free parameters* which, because of its 3-d character, constitutes a considerable improvement over the classical Landau solution. Using two different equations of state (eos) - one containing a phase transition from QGP to the Hadronic Phase and two versions of a purely hadronic eos - we find that the first one gives an overall better description of the $Au + Au$ experimental data at AGS energies. We reproduce and analyse measured meson and proton spectra and also make predictions for anti-protons, deltas, anti-deltas and hyperons. The low m_t enhancement in π^- spectra is explained by baryon number conservation and strangeness equilibration. We also find that negative kaon data are more sensitive to the eos, as well as the K^-/π^- ratio. All hyperons and deltas are sensitive to the presence of a phase transition in the forward rapidity region. $\bar{p}$, Ω and

*E. Mail: ARBEX@MAILER.UNI-MARBURG.DE

†E. Mail: ORNIK@WARP.SOULTEK.DE

‡E. Mail: PLUEMER@MAILER.UNI-MARBURG.DE

§E. Mail: WEINER@MAILER.UNI-MARBURG.DE

heavy anti-baryons are sensitive in the whole rapidity range.

PACS numbers: 24.10.Nz, 25.75.-q, 25.75.Dw

1 Introduction

Two main conclusions can be drawn so far from the study of heavy ion reactions at AGS and SPS accelerators:

(i) nuclear matter is not transparent [1]. In particular for collisions of heavy nuclei at AGS ($Au + Au$) the shape of the proton rapidity density distribution around the center-of-mass rapidity suggests an almost total nuclear stopping [2], which also means that high baryon densities are achieved [3].

(ii) The assumption of local thermodynamical equilibrium leads to an astonishing agreement with the data. This follows among other things from the fact that simple fireball models [4],[5] which take into account a longitudinal flow component can explain many features of the data.

These aspects justify the investigation of heavy ion physics with more realistic hydrodynamical models which - if applicable - would serve as a powerful tool for the description of strongly interacting many particle systems and hadronic multiparticle production ([6]-[11]).

The basic hydrodynamical model is a generalization of statistical models introduced in the early fifties [13]. It was introduced by Pomeranchuck and Landau [14]-[18] who removed several weak points of the previous fireball models. The unrealistic concept of a fireball in global equilibrium, which is not consistent with the covariant relativistic dynamics of the collision, was replaced by the concept of a system in local equilibrium.

The latter concept is more general and takes into account that the whole system is not yet completely equilibrated, but has inhomogeneities caused by the initial dynamics, which are controled by the strong interaction. It also takes into account that a system at very high temperatures does not only evaporate particles from the surface but also has to expand because of the strong internal pressure. The details of the expansion are determined by the equation of state (eos), which describes the properties of strongly

interacting hot hadronic matter.

The expansion leads to a cooling of the system which changes the absolute particle yields, the chemical composition of the fireball (particle ratios), the momentum distributions, as well as the mean free path, which increases with decreasing density (or temperature) of the system. If the mean free path is large enough the particles decouple (freeze-out) from the fireball.

The concept of local equilibrium and relativistic covariance also requires that decoupling takes place locally, i.e. the particles are emitted when the fluid cell reaches the decoupling temperature T_f [1]. In other words, below T_f the mean free path becomes too large in order to maintain equilibrium. A local freeze-out usually leads to a very complicated shape of the emission region in space-time (the freeze-out hypersurface).

From the hydrodynamical point of view it is convenient to divide a heavy ion collision into 3 stages:

1. The compression and thermalization of nuclear matter forming the locally equilibrated fireball (*compression stage*).

2. The hydrodynamical expansion of the fireball (*expansion stage*).

3. The decoupling of particles (*freeze-out*).

Supported by the observation of a high amount of stopping, we have extended the 3-d hydrodynamical description to the very beginning of the fireball formation process. The applicability of the numerical code HYLANDER [19], which exactly solves the relativistic hydrodynamical equations (Eq.1) and which we used in, e.g. [9], [10],[12], is now amplified to simulate the whole collision, from the very moment the two nuclei touch each other.

The purpose of this work is: 1) to apply the above hydrodynamical formalism to $Au + Au$ reactions at AGS in order to investigate the eos as well as the possibility of a

---

[1]In this work we choose a critical temperature T_f on the order of the pion mass for the freeze-out criterion.

4

phase transition and 2) to make predictions for yet unobserved particle species and their spectra.

The paper is organized as follows. In Sec. 2 we introduce the equations of state under investigation. In Sec. 3 we describe the hydrodynamical model. In Sec. 4 the results of the simulations are shown. It contains an analysis of the equations of state and the corresponding properties of the simulated fireballs, and the comparison with published data for protons, pions and kaons, as well as predictions for anti-protons, heavy baryons and heavy anti-baryons. In Sec. 5 we present a description for the negative pion enhancement and discuss strange particle rates. Sec. 6 contains a discussion of our results.

2 Hydrodynamical Model

In their simplest form the hydrodynamical equations do not include dissipative effects. The incorporation of dissipation in a relativistically covariant way is up to now very difficult and requires approximations. Some progress in this field has been made for two and three fluid dynamics and dissipative shock waves [20]-[23]. In the following we will restrict ourselves to one fluid described by the relativistic Euler equations,

$$
\begin{aligned}
\frac{\partial E}{\partial t} &= -\nabla\left((E+P)\mathbf{v}\right) && \text{energy conservation} \\
\frac{\partial M^i}{\partial t} &= -\nabla(M^i\mathbf{v}) - \frac{\partial P}{\partial x_i} && \text{momentum conservation} \\
\frac{\partial(b\gamma)}{\partial t} &= -\nabla b\mathbf{v} && \text{baryon number conservation} \\
E &= \gamma^2(\varepsilon + Pv^2) \\
\mathbf{M} &= \gamma^2(\varepsilon + P)\mathbf{v}
\end{aligned}
$$

(1)

where $\mathbf{v}(\vec{x}, t)$ is the velocity of the fluid, $\gamma = 1/\sqrt{1 - v^2}$, P is the pressure, ε is the

5

energy density and b is the baryon density.

The solution of these equations is determined by the equation of state which can be written in the form

$$P = P(\varepsilon, \mu), \tag{2}$$

where μ is the chemical potential. It governs the compression, the expansion and the freeze-out surface shape of the fireball.

If the local density drops below a critical value (ρ_f) the particles are assumed to decouple (locally) from the fluid, i. e. hydrodynamics is not applicable beyond this point. The primordial resulting particle spectra are then described by the Cooper-Frye formula [24]:

$$E\frac{dN}{d\vec{p}} = \frac{g_i}{(2\pi)^3} \int_\sigma \frac{P_\mu d\sigma^\mu}{exp(\frac{P_\mu u^\mu - \mu_s - \mu_b}{T_f}) \pm 1}, \tag{3}$$

which describes the distribution of particles with degeneration factor g_i and 4-momentum P^μ emitted from a hypersurface element $d\sigma^\mu$ with 4-velocity u^μ. After the cascading of the resonances we obtain the final observable spectra.

In our earlier approach [9] at SPS energies we took into account that due to transparency effects the local equilibrium state is reached after undergoing a non-equilibrium stage, which is not treatable with hydrodynamics. Therefore we started our simulation in an intermediate state which we had to model by introducing some parameters based on "reasonable" assumptions about the initial configuration. However both for $S + S$ and $Pb + Pb$ [12] collisions we found that the inelasticity necessary to describe the data was larger than 70%. For lower energies (AGS) the inelasticity (or amount of stopping) is expected to increase.

Therefore in the present paper we extend the HYLANDER-code using a different ap-

proach to the hydrodynamics of heavy ion collisions suited for processes with (almost) full-stopping. It is based on the original Landau model [14],[15] where the process of stopping is also treated hydrodynamically, rather than being parametrized by some initial conditions as in [9],[10]. As will be explained below, our approach constitutes an important improvement over the old Landau approach as it eliminates all approximations he made.

The starting point of the model are two colliding tubes at zero temperature and nuclear ground state density. The width in longitudinal (beam) direction is given by the Lorentz-contracted nuclear diameter in the equal velocity frame. This problem was solved by Landau analytically [14] with the following approximations:

1. the assumption of 1-dimensional shock waves,

2. the 1-d hydrodynamical description for the beginning of the expansion process followed by an approximated 3-d analytical solution and

3. an equation of state of the type $P = c_0^2 \varepsilon$ where c_0 is the constant velocity of sound.

In the present work we do not use any of these approximations, since both the *compression stage* and the *expansion stage* are described by a fully 3-dimensional hydrodynamical simulation.

As a consequence we have additional contributions to the particle spectra from the very early *compression stage*. The $Au + Au$ system at AGS spends about 4 fm/c in this stage[2].

Given the fact that, due to this treatment, there are no free parameters necessary to describe the initial conditions of the fireball, it becomes now possible to study the

---

[2] Landau made an $1-d$ approximation of these stage and neglected its contribution to the spectra. Such a method is only justified at extremely high energies where the Lorentz contracted longitudinal diameters before collision are very small compared to the lifetime of the system, which is not the case for AGS energies. Squeeze-out effects and transverse motion are also not present in Landau's approach.

sensitivity of the results to the properties of the eos. This will be done by applying our solutions of 3-d hydrodynamics to $Au + Au$ reaction at the AGS.

3   The Equations of State

In this work we considered two models for the eos as an input to solve numerically the relativistic hydrodynamic equations with the HYLANDER code:

1) Firstly we present an eos given by a parametrization [25] of lattice-QCD results [26]. It describes a first order phase transition between quark gluon plasma and hadronic matter at $T = 200MeV$ and corresponds to a baryon chemical potential $\mu = 0$ [3]. The baryons are explicitly considered in the hydrodynamical equations. We will refer to this eos as **lattice-eos**.

2) Secondly we took two versions of a resonance gas equation of state [20],[28], which differ in the number of included resonances. In the following we will refer to **RG1.5** for a resonance gas including resonances with masses up to 1.5 GeV and **RG2** for a gas of resonances of masses up to 2 GeV. In this eos the dependence on the baryon chemical potential and strangeness conservation is included.

4   Results

4.1   Energy density, baryon density and lifetime

Table 1 shows the values for maximum energy density, maximum baryon density and the time it takes until the fireball is completely transformed into free particles (lifetime). All these simulations start at the moment of the impact between the nuclei ($t = 0$).

---

[3]In [26] a pure gluonic system is considered. Results considering dynamical quarks lead to a critical temperature T_c between 150 and $200MeV$ [27].

The system spends one third of its lifetime in the compression stage, confirming the importance of this part of the process.

The values for lifetime, maximum baryon and energy density for lattice-eos and RG2 are surprinsingly similar, but this does not necessarily mean that the behaviour of each fluid cell (and of the whole fluid) until freeze-out is also the same. To investigate this we study the trajectory of the fluid elements in a phase diagram of energy density versus temperature, for the three eos (see Fig.1). In this figure we plot the temperature and energy density for each fluid cell with $T > 139\ MeV$ (which means for all $\vec{x}$ and t), starting at the beginning of the simulation.

One sees that for lattice and RG2 the fluid elements describe a trajectory in almost the same energy density and temperature range. For both simulations the fluid elements can reach temperatures up to 215 MeV and energy densities bigger than 6 GeV/fm^3, for lattice-eos this correspond to temperatures slightly above the phase transition temperature.

The trajectory for RG1.5 is located in a very different range. The explicit dependence on a baryonic chemical potential in RG2 and RG1.5 appears just in the "width" of the curve. It is interesting to note that even in the case of RG1.5 and RG2 where μ enters explicitly in the calculation the baryon dependence is weak, i.e. the "width" of these curves is surprisingly small.

The similarity in the results for energy density, baryon density and lifetime for lattice-eos and RG2 can be explained by Hagedorn's model [28]. Increasing the number of resonances in the hadronic gas eos induces a phase transition-like behavior in the development of the fireball [4].

---

[4] An important and obvious question is whether this behaviour of the fluid elements will be the same for other nuclear reactions. We performed a simulation for $Pb + Pb$ at 160 $GeV/nucleon$ to try to answer this question. We used the same initial condition as in the present paper and two eos, namely lattice and RG2. The resulting trajectory of the fluid elements differs from that for the AGS system. The difference between both eos appears for temperatures larger then 0.2 GeV. What this implies for the particle spectra

The sensitivity of the produced particle spectra to these differences in the eos is the subject of the following sub-sections.

4.2 Particle spectra

At freeze-out temperature we treat explicitly the emission of protons, neutrons, pions, kaons, anti-protons (directly produced) and the particles/resonances: $\Omega(783)$,η,$\eta\prime$, ρ,K_0,K^*, Δ,Σ,Λ,Ξ and correspondent anti-particles (see [9]). The results we present in the next sub-section take into account the contribution from the decay of particles.

4.2.1 Spectra of protons, pions and kaons

In Figure 2 we compare the transverse mass $(m_t = \sqrt{m^2 + p_t^2})$ spectra of protons, positive and negative pions for different rapidity intervals from our **RG1.5** simulation with experimental data [2],[3]. All spectra obtained for this eos differ considerably from the data.

In Figure 3 we show the corresponding results from our simulation using the **lattice-eos**. One can see that, except for the very central region (last curve), where the proton production is overestimated, the experimental proton spectra are very well fitted. The fits for positive and negative pions show the same tendency: significant deviation from the data we observed only in the very central rapidity region (first curve). In all cases there is a small overestimate of particle production at large p_t, which means in hydrodynamical terms an overprediction of transverse flow.

In the last section we mentioned the similarity in the lifetime, baryon and energy density, as well as the trajectory of the fluid elements arising from lattice-eos and RG2 simulations. Therefore we expect that the RG2 spectra are more similar to the spectra obtained using lattice-eos than to the ones using RG1.5.

The simulation using RG2 confirmed this expectation. One can see this in Figure 4

will be discussed elsewhere [29].

10

where we consider the m_t spectra resulting from the simulation with **RG2**. Particularly for pions we observe a very good agreement with the data. Even the overestimate of pions at large p_t observed for the lattice-eos simulation vanishes. In the case of protons we observe deviations only in the very central rapidity region.

In Figure 5 we compare the spectra, at fixed rapidity, for all three simulations. Here one can see that for the protons the best fit is clearly given by the lattice-eos simulation. For positive pions the simulation by RG2 is better and for negative pions the best results are obtained with both lattice-eos and RG2.

If we take into account the so far available data we can already conclude that a medium with a large number of internal degrees of freedom (a very "soft" eos) is favoured.

All three simulations show at midrapidity an overestimate of proton and pion yields. We attribute this effect to the transverse squeeze-out of nuclear matter which has its maximum at zero impact parameter (central collisions). We recall that the data are sampled over a finite impact parameter (b) region [5] , whereas the simulation is really at $b = 0$, therefore the squeeze-out appears diluted in the data.

However we do not encounter the problem cited in [2] (and references quoted there for Monte Carlo models) which could not reproduce the flatness and shape of the proton and pion spectra.

The enhancement at low m_t exhibited in the π^- spectra is present in all three simulations. We can reproduce this effect in a natural way just by taking into account resonances, baryon conservation and strangeness equilibration, without invoking statistical and systematic errors in the data, as was done in [3]. This manifests itself not only as a change in the shape of the π^- spectra but also as an increase of the total multiplicity of negative pions compared to the positive ones. A more precise analysis of π^- and π^+ production will be presented in section 4.4.

---

[5] The "very central" data (4% centrality) for $Au + Au$ AGS correspond to an impact parameter $b < 2.6$ fm (Y.Akiba, private communication and QM96).

Now we turn to rapidity distributions [6] (Fig. 6).

For protons and pions the already observed tendency is confirmed, namely the results arising from the simulations with lattice-eos and RG2 are closer to the data than RG1.5.

In pion production one can see here explicitly that the hydrodynamical simulation produces more negative pions than positive ones, a fact which is confirmed by the experiment.

In the rapidity distribution analysis we include a comparison between our results and strange particle production data. This is of particular importance because of the well known proposal to look at strangeness production as a signature of QGP (cf. e.g. [31] - [34] for more recent references).

In Figure 6 one also can see that for the kaon rapidity spectra the difference between the three simulations is more pronounced, particularly for negative kaons. The comparison with preliminary data favours the lattice-eos.

As an preliminary conclusion for this sub-section we can say that the results are generally in surprisingly good agreement with the data, especially if one takes into account that we do not need any parameters other than those that enter the eos.

We also see that the presence or absence of a phase transition can not be determined by the analysis of m_t spectra of protons and pions.

The situation appears to be different if we look at other aspects such as the total number of produced protons and pions (see Table 2) and the rapidity distributions of protons, pions and especially kaons, where we observe remarkable differences between the spectra resulting from the three simulations.

Since kaon production in a baryon-rich medium is linked to hyperon production and chemical equilibration we expect from those also a sensitivity in the hyperon yield related to the eos. Motivated by this fact we will investigate in the following the rapidity dis-

---

[6] The rapidity distributions from our model do not contain the phase space cuts at low m_t which are present in the data.

tributions of deltas, hyperons and their corresponding anti-particles. We also consider anti-proton production.

The data are generally better described if one uses a "softer" eos. Because of that from now on we will restrict the discussion to the results from the simulations with the lattice-eos and RG2.

4.2.2 Predictions for anti-baryons and heavy baryon production

In Figures 7,8 and 9 we show the rapidity distributions for anti-protons, heavy baryon and heavy anti-baryon production. Table 2 shows the total particle number for all created particles and anti-particles for the three simulations.

The lattice-eos produces a larger or a comparable number of heavy baryons and heavy anti-baryons than RG2 (except for Δ). The largest differences are predicted for Ξ, Ω, $\bar{\Delta}$ and $\bar{p}$ [7].

For heavy baryons (Fig. 8) differences appear in the forward rapidity spectra ($y > 1.0$). The Ω production differs in the whole rapidity range. For the heavy anti-baryons rapidity spectra (Fig.9) differences appear in the whole rapidity range, except for $\bar{\bar{\Xi}}$, where the difference appears only in the forward region ($y > 1.0$).

5   Highlights

In the following we would like to emphasize three remarkable results of our calculations: (a) the enhanced π^- production compared with π^+ production; (b) the ratio N_{Ξ^-}/N_Λ; and c) the rate K/π.

a) Taking into account baryon and strangeness conservation as well as strangeness equilibration at AGS energies and including the decay of the resonances in the final stage in

---

[7]The direct $\bar{p}$ production contributes with only $\sim 30\%$ to the total $\bar{p}$ abundancy total numbers.

our model the difference $N_{\pi^-} - N_{\pi^+}$ is given by

$$N_{\pi^-} - N_{\pi^+} = 0.64 N_\Lambda + N_{\Sigma^-} + N_{\Xi^-} + 0.64 N_{\Xi^0},$$

i.e., the hyperons and their decay mainly determine the difference between π^- and π^+ total numbers. Since our model fits both the π^- and π^+ spectra, we have a natural and simple explanation for the experimentally observed difference in the multiplicities of positive and negative pions. This also explains the experimental observation from flow analysis that π^- flow is correlated with the protons [8], as the π^- contribution from hyperon decays is connected to the baryon flow[9].

b) In [37] multi-strange hyperons ($S \geq 2$) and strangelets are suggested as better signatures than single-strange particles ($S = 1$). The first report about Ξ^- production in heavy ion collisions at AGS [38] (for $Si + Pb$) mentions that the observed rates are at least 5 time bigger than all present cascade model predictions. There are no such data avaiable for $Au + Au$ collisions at AGS energies at the moment, but $Si + Pb$ at AGS energies constitutes an experiment in the same energy range, with a high baryon density and a high amount of stopping. Encouraged by these aspects we compare our results with these data.

For $Au + Au$ we find the following results:

$N_{\Xi^-}/N_\Lambda = 0.126$ (lattice-eos)

$N_{\Xi^-}/N_\Lambda = 0.090$ (RG2)

which are in agreement with the experimental value of 0.12 ± 0.02 for $Si + Pb(AGS)$. However the difference between lattice-eos and RG2 simulations is not very big which leads us to the tentative conclusion that the Ξ^- production does not necessarily serve as

---

[8]T.Hemmick private communication and QM96.

[9] In reference [36] the authors investigate the low m_t enhancement in π^- production for $Pb+Pb$ system at SPS energies and attribute it to the Coulomb effect. It is likely that the explanation presented above for the AGS data applies in this case too. Results on this subject will be presented elsewhere. This sugests that the Coulomb effect invoked to explain these data is probably much weaker than assumed in [3][36].

a better signal for QGP than other strange particle yields.

c) The experimental ratios K/π for $Si + Au$ (AGS) were measured and published in [39]. The values are $K^+/\pi^+ = 0.192 \pm 0.03$ and $K^-/\pi^- = 0.036 \pm 0.008$ in the mid-rapidity region and they have been presented as intriguing results because of the large strangeness yields compared with $S + S$ (SPS), where both values are about 0.11. For $Au + Au$ (AGS) experiment the ratio K^+/π^+ is found to be 0.21 [3] and the negative ratio was not yet published.

The results are remarkable in the sense that there are no strange particles present in the initial state and a significant rate of strange particle production is only understandable if a strange chemical equilibrium is established during the reaction. Strangeness equilibration however is not easy to justify in a pure hadronic scenario.

From our calculations, which includes the assumption of strangeness equilibrium, we find:

$N_{K^+}/N_{\pi^+} = 0.207$ (lattice-eos) and 0.256 (RG2),

which are in surprisingly good agreement with the experimental results, especially for the lattice-eos scenario. The numbers from the lattice-eos and RG2 simulation are not very different and we can conclude therefore that this result is a strong indication of local equilibration (including strangeness equilibrium) of the system. The signal however is not very sensitive to the concrete type of the eos.

On the other side, clear differences appear (see Table 2) for the other ratio: $N_{K^-}/N_{\pi^-} = 0.038$ (lattice-eos) and 0.018 (RG2). Experimental information about this ratio is very important and should be treated with care.

From our results we can conclude that a hadronic scenario considering strangeness equilibration can also explain the difference between the positive and the negative ratios [10].

---

[10]Other aspects in this discussion related to $Si + Au$ (AGS) is presented in [40]

6 Conclusions

We have demonstrated that the 3d-hydrodynamical model presented above can describe quite reasonably the AGS data for $Au + Au$ reactions. This suggests that the hypothesis of local thermodynamical equilibrium applies also for the early stage of the reaction.

We showed that both an eos based on QCD lattice calculations exhibiting a phase transition between quark gluon plasma/hadronic phase (lattice-eos) and a resonance gas eos including resonances with masses up to 2 GeV (RG2) have the essential physical properties necessary to describe the mesured proton and pion m_t spectra. An eos described by a resonance gas with a small number of degrees of freedom (RG1.5) is not consistent with these data. However as shown by Hagedorn [28] the RG2 scenario is related to the idea of a phase transition. This phase transition-like behaviour becomes even more pronounced if one adds higher resonances. However, we note that the assumption of strange chemical equilibration , which is assumed to be present even in this hadronic scenario, is not easy to justify in the case of a pure hadronic eos.

In a general analysis including the m_t spectra for protons and pions, the total multiplicities of produced protons and pions and their rapidity distributions we can conclude that the lattice-eos provides an overall better description of the $Au + Au$ (AGS) experimental data than a hadronic eos.

We have also calculated the particle spectra for anti-baryons and heavy anti-baryons and the rates π/K and Ξ^-/Λ in order to investigate the influence of a phase transition on the production of these particle species.

Generally the simulation with the equation of state containing a QGP-hadronic phase transition between a hadronic phase and a QGP predicts a larger total multiplicity of heavy baryons and anti-baryons than with resonance gas. The largest differences in the number of produced particles appear for Ξ, Ω, $\bar{p}$ and $\bar{\Delta}$.

In all heavy baryon and heavy anti-baryon rapidity distributions, the strong difference

16

between both eos scenarios appears in the forward region of rapidity, $y > 1.0$. For Ω and heavy anti-baryons (except for $\bar{\Xi}$) differences are also predicted in the mid-rapidity interval. Despite the lower multiplicities this could be an interesting topic for future experiments.

Negative kaons we found to be more sensitive to the presence of a phase transition in the eos than the positives ones, as well as the corresponding K^-/π^- ratio. The ratio K^+/π^+ has been compared with experimental data and and both scenarios (specially the lattice one) are in good agreement with the measured ratios, a fact which again supports the assumption of an almost complete chemical equilibration. Differences between the positive and the negative ratios were found in both scenarios.

The rate Ξ^-/Λ was compared with experimental data (for $Si + Pb$) and is in good with them. The results for both scenarios are not very different and therefore we conclude this ratio involving a multi-strange hyperon does not appear to be a better signature then the $S = 1$ particle yields.

A particularly important aspect of our investigation is that the high negative pion multiplicity in this experiment can be obtained in a natural way just taking into account baryon and strangeness conservation, strangeness equilibration and resonance decays. It has its origin mainly in the Λ, Σ and Ξ channels, as we showed in detail in the previous section. The low m_t enhancement in π^- spectra can also be explained in this way. We conclude that, contrary to the statement made in [36], the Coulomb effect does not strongly affect the pion spectra.

Another step in the investigation of the equation of state which governs the heavy ions physics would be to realize the same simulation using an eos based on lattice-QCD calculations extended into the baryonic sector.

References

[1] see for example: J.Stachel and P.Braun-Munzinger, Phys. Lett. B 216(1989)1; E814/E877 Collaboration, Phys. Rev. Lett. 70(1993)2996.

[2] BNL-AGS E802/866 Collaboration, Nucl.Phys. A590 (1995) 519c.

[3] J.Barrette et al., Nucl.Phys. A590 (1995) 249c.

[4] E.Schnedermann, J.Sollfrank and U.Heinz, Phys. Rev. C48(1993)2462.

[5] P.Braun-Munzinger, J.Stachel, J.P.Wessels and N.Xu, Phys. Lett. B344(1995)43.

[6] R.B.Clare and D.Strottman, Phys.Reports 141(1986)177.

[7] R.Waldhauser, D.H.Rischkem, U.Katsher, J.A.Maruhn, H.Stoecker and W.Greiner; Z. Phys. C54(1992)459.

[8] U.Ornik, F.Pottag and R.Weiner, Phys. Rev. Lett. B63(1989)2641.

[9] J.Bolz, U.Ornik, R.W.Weiner; Phys.Rev.C 46(1992)2047.

[10] J.Bolz, U.Ornik, M.Plümer, B.R.Schlei and R.Weiner; Phys.Lett B300(1993)404; Phys.Rew. D47(1993)3860.

[11] for a recent review see D.Strottman, Nucl. Phys. A566(1994)245c.

[12] 'Hydrodynamical analysis of single inclusive spectra and Bose-Einstein correlations for Pb+Pb at 160 GeV'; U.Ornik, M.Plümer,B.Schlei,D.Strottman,R.Weiner; submitted to Phys. Lett.B.

[13] E. Fermi, Prog.Th.Phys., 1950

[14] L.D.Landau; Izv.Akad.Nauk.(USRR) 17(1953)51.

[15] Collected Papers of Landau; Pergamon Press, 1965, n.88.

[16] I.Y.Pomeranchuck; Dokl.Akad.Nauk.(USRR) 78(1951)889.

[17] S.Z.Belenkij and L.D.Landau; Fiz.Nauk. 56(1955)309.

[18] S.Z.Belenkij and G.A.Milekin; Zh.Eksp.Theor.Fiz. 29 (1955)20; Sov.Phys.-JEPP 2(1976)14.

[19] PhD thesis, "Relativistische Hydrodynamik mit Phaseübergang in der Kosmologie und in Kern-Kern-Stössen", U.Ornik, Marburg Universitaet, 1990.

[20] L.Mornas and U.Ornik, Nucl. Phys. A587(1995)828.

[21] P.Danielewicz, Phys.Lett. B 146(1984)168.

[22] M.S.Ganagi and A.V.Gopalakrishna, Astrophys. Spa. Sci. 129(1987)281.

[23] M.P.Galipo, Lett. Nuov. Cim. 38(1983)233,427,544.

[24] F.Cooper,G.Frye and E.Schonberg; Phys.Rev.D 11(1975)192.

[25] U.Ornik, F.W.Pottag, R.W.Weiner; Phys. Rev. Lett. 63(1989) 2641.

[26] K. Redlich and H.Satz, Phys. Rev. D33(1986)3747.

[27] T. Blum, T.DeGrand, C.DeTar, S.Gottlieb, A.Hasenfratz, L. Kärkkäinen, D.Toussaint and R.L.Sugar; Phys. Rew. D50 (1994) 3377 and references therein.

[28] R.Hagedorn, Nuov. Cim. Suppl. 3(1965)147; J.Rafelski and R. Hagedorn, Bielefeld Symp., 1980, ed. H.Satz, pg.253.

[29] 'The Phase Transition in the SPS Energy Range', in preparation, N.Arbex, U.Ornik, M.Plümer, B.Schlei and R. Weiner.

[30] Review of Particle Properties; Particle Data Group, Phys. Lett. B204 (1988).

[31] R.Stock, GSI-Yellow Report, Darmstad 1981.

[32] T.A.DeGrand, Phys. Rew. D30(1984)2001.

[33] P.Koch, B. Mueller and J.Rafelski, Phys.Rep.142 (1986)167.

[34] K.S.Lee, M. Rhoades-Brown and U.Heinz, Phys.Rew. C37(1988)1452.

[35] 'Space-time development of AGS fireball- Correlation Functions and 3-d Hydro-dynamical Model', in preparation; N.Arbex, U.Ornik, M.Plümer, B.Schlei and R. Weiner.

[36] 'Coulomb Effect in Single-Particle Distributions', H.Boggild et al.; CERN-PPE/96-02, submitted to Phys.LettB).

[37] C.Greiner, P.Koch and H.Stöcker; Phys. Rev. Lett 58(1987)1825.

[38] S.E.Eiseman et al., Phys. Lett. B325(1994)322.

[39] T.Abbott et al.; Nucl. Phys. A498(1989)67c

[40] J.Cleymans, H.Satz, E.Suhonen and D.W. Von Oertzen; Phys. Lett B242(1990)111.

Figure Captions

Fig. 1: Plot of temperature and energy density of each fluid cell with $T > 139\ GeV$, from the beginning of the collision, for the hydrodynamical simulation (HYLANDER) using the different eos. The figure shows the trajectory of the cells in the (ϵ, T) diagram until they freeze out. a)for RG1.5, b) for lattice-eos and c) for RG2.

Fig. 2: Transverse mass spectra for five rapidity intervals for protons, positive and negative pions using the equation of state RG1.5. The data (taken from [3] [2]) and hydrodynamical simulated curves obtained for hydrodynamical simulation (HYLANDER) are shown for rapidity bins from 1.7 to 2.5 (for pions), from 0.9 to 1.7 (for protons). In both cases the bin size is 0.2 and the bins are centred around $y_{central} = 1.6$.

Fig. 3: Transverse mass spectra for five rapidity intervals for protons, positive and negative pions using lattice eos. The data and rapidity intervals are the same as in Fig. 2.

Fig. 4: Transverse mass spectra for five rapidity intervals for protons, positive and negative pions using RG2. The rapidity intervals and data are the same as in Fig. 2 and 3.

Fig. 5: Comparison of the m_t spectra at fixed rapidity ($y = 2.1$ for pions and $y = 1.3$ for protons) for hydrodynamical simulations (HYLANDER) using lattice, RG2 and RG1.5 equations of state.

Fig. 6: Rapitity distribution for protons, pions and kaons for hydrodynamical simulations (HYLANDER) using lattice, RG2 and RG1.5. equations of state. The data are from [3].

Fig. 7: Rapidity distribution for anti-protons for hydrodynamical simulations (HYLANDER) using lattice and RG2.

Fig. 8: Rapidity distribution for heavy baryon production ($\Delta, \Sigma, \Lambda, \Omega$ and Ξ) for hydrodynamical simulations (HYLANDER) using lattice and RG2.

Fig. 9: Rapidity distribution for anti-baryons production ($\bar{\Delta}, \bar{\Sigma}, \bar{\Lambda}, \bar{\Omega}$ and $\bar{\Xi}$) for hy-

drodynamical simulations (HYLANDER) using lattice and RG2.

Table Captions

Table 1: Maximum values for energy density, baryon density and lifetime for hydrodynamical simulations (HYLANDER) using three different eos. n_0 is the normal baryon density.

Table 2: Total multiplicities of produced particles and anti-particles from simulations using the three different eos. The numbers take into account the shown isospin degeneracy factors. The data are from [3] (The error bars are around 10%. Y.Akiba, private communication) .

Table 1

	lattice eos	RG2	RG1.5
max. energy density	6.6 GeV/fm^3	7.5 GeV/fm^3	2.5 GeV/fm^3
max. baryon density	13.6 n_0	16.7 n_0	5.6 n_0
lifetime	10 fm/c	10 fm/c	15 fm/c

Table 2

particle	lattice eos	RG2	deg. factor	data
p	132.800	140.200	1	160
π^+	140.200	100.800	1	115
π^-	155.000	109.000	1	160
K^+	29.000	25.800	1	-
K^-	6.000	2.000	1	-
Ξ	4.100	2.400	2	-
Δ	153.300	197.600	4	-
Λ	16.200	13.700	1	-
Ω	0.200	0.080	1	-
Σ	31.300	26.800	3	-
$\bar{p}$	0.200	0.100	1	-
$\bar{\Xi}$	0.075	0.080	2	-
$\bar{\Delta}$	0.095	0.044	4	-
$\bar{\Lambda}$	0.055	0.036	1	-
$\bar{\Omega}$	0.020	0.030	1	-
$\bar{\Sigma}$	0.100	0.070	3	-

FIGURE 1
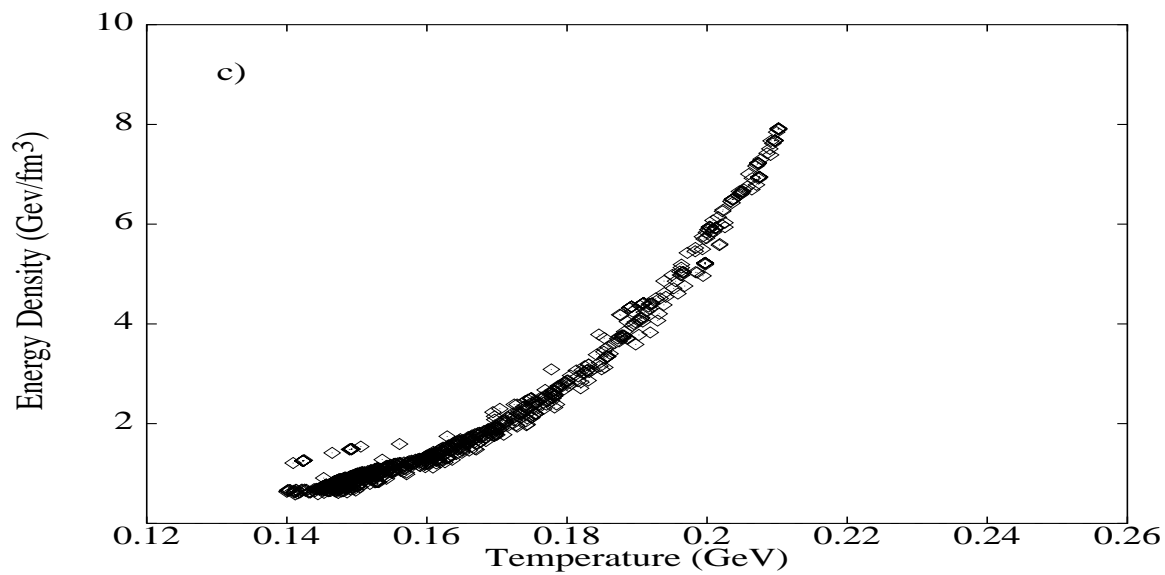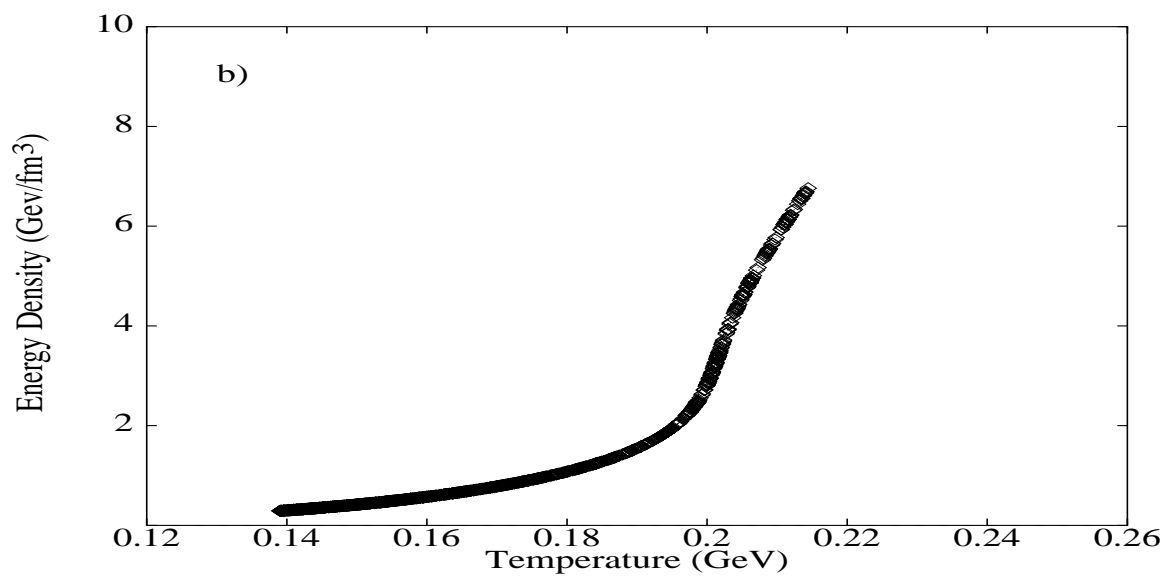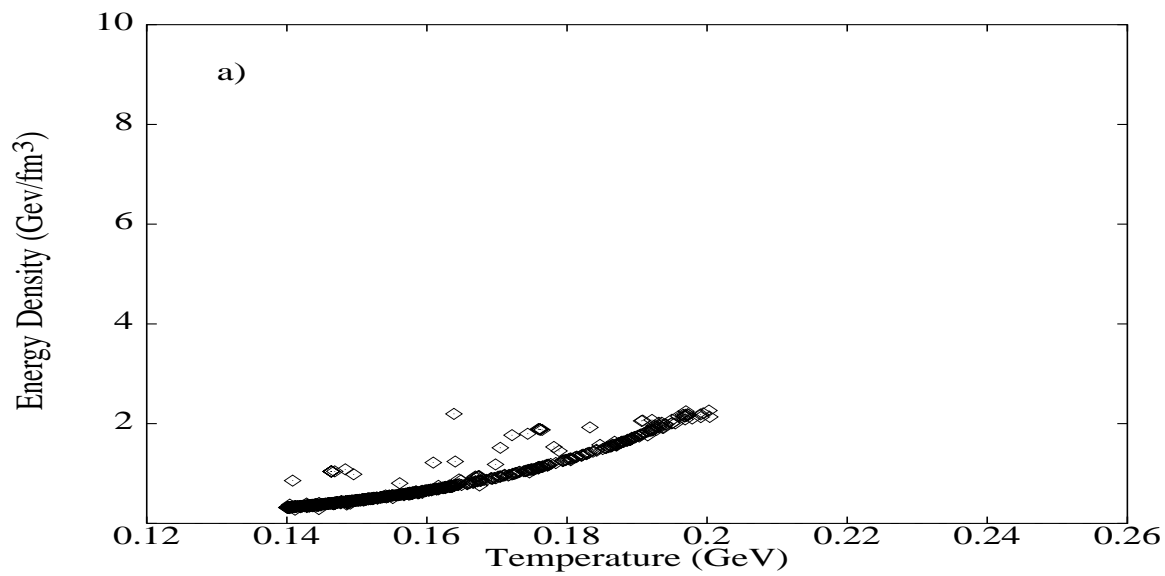
FIGURE 2
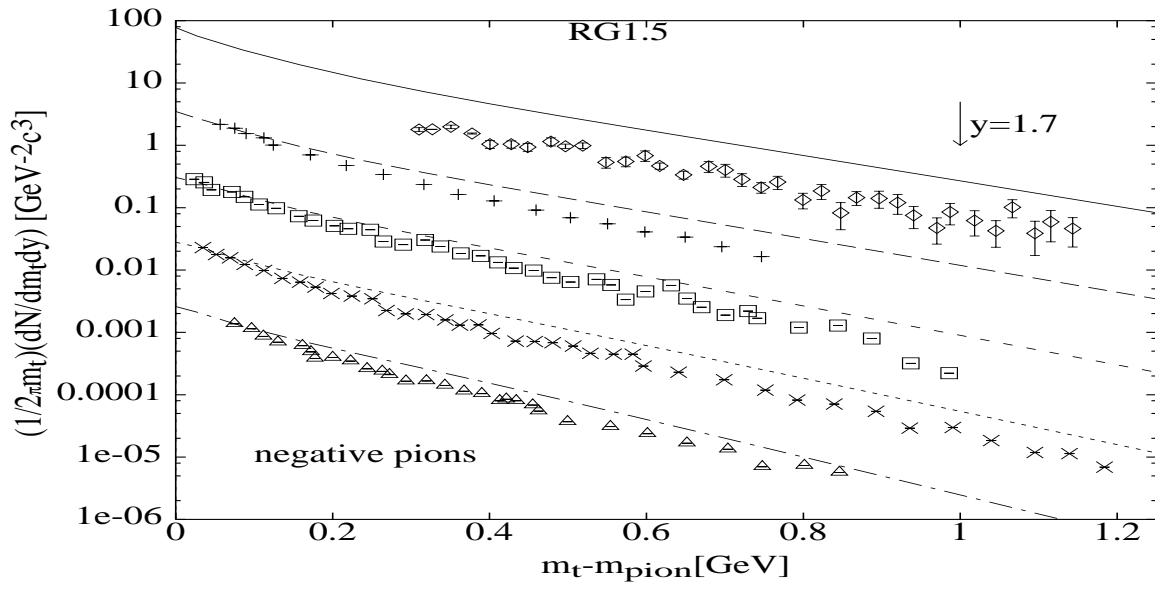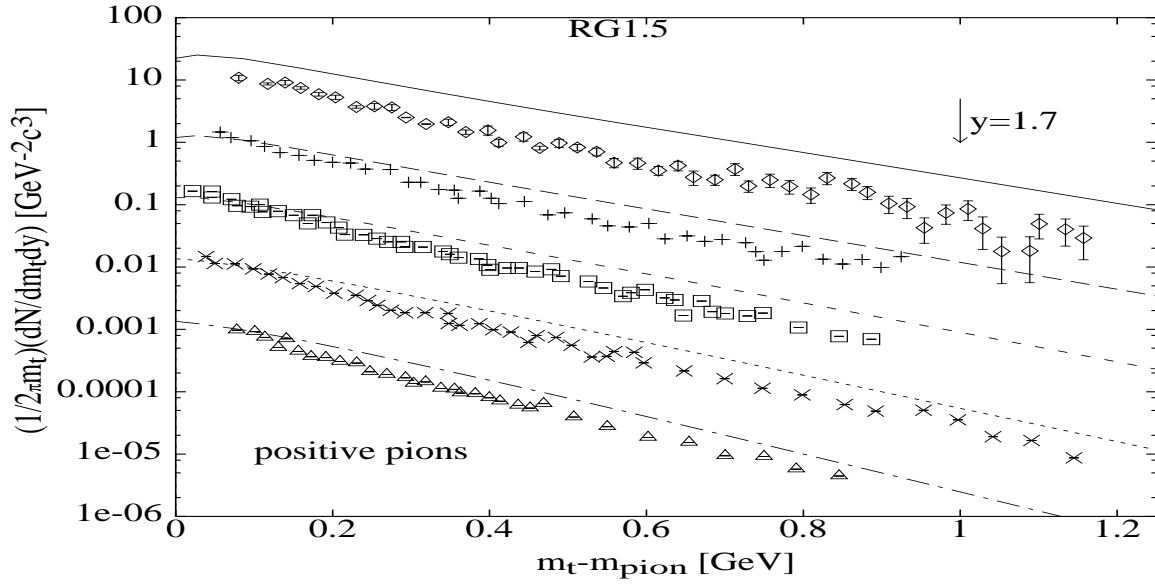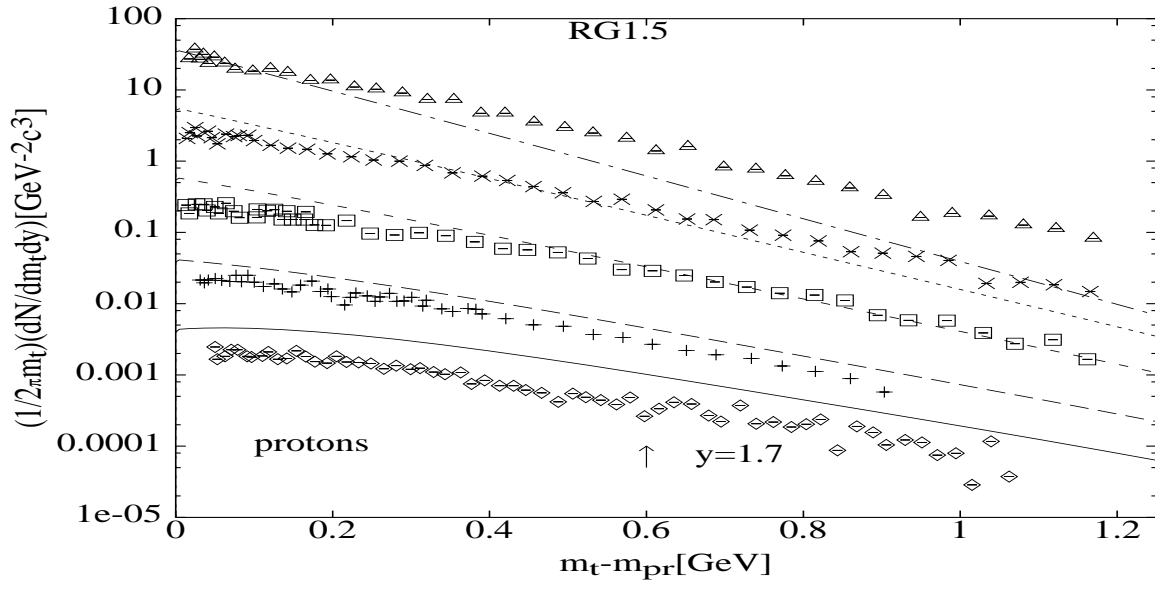
FIGURE 3
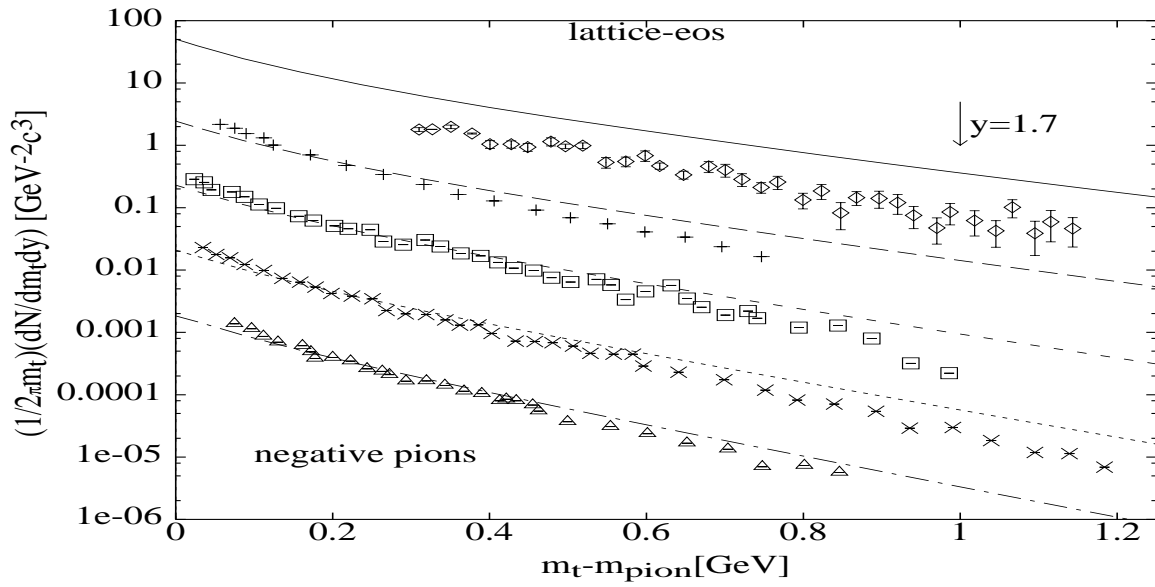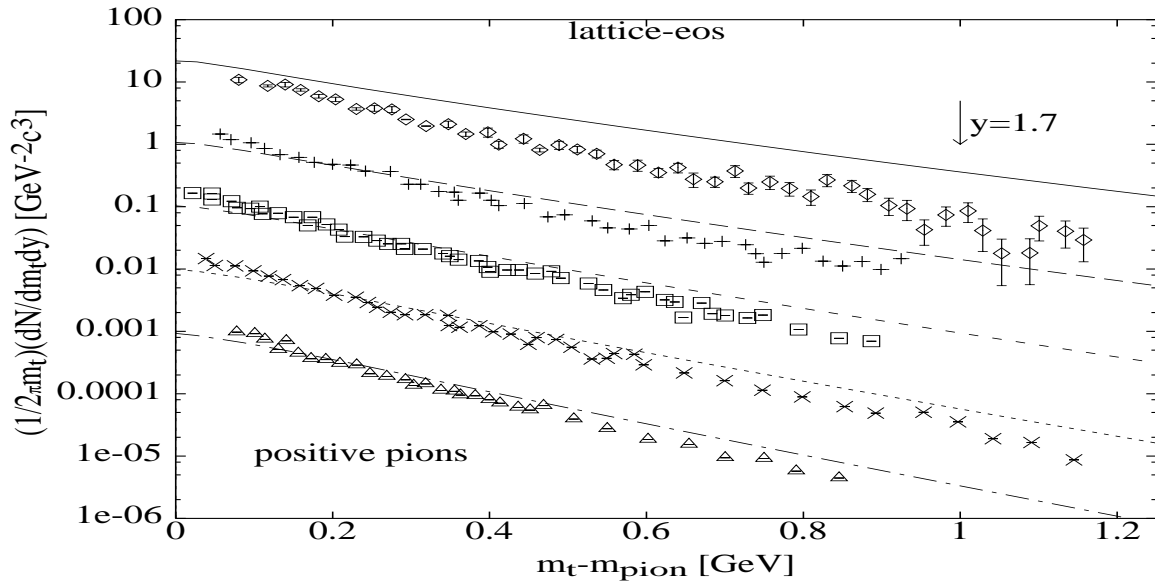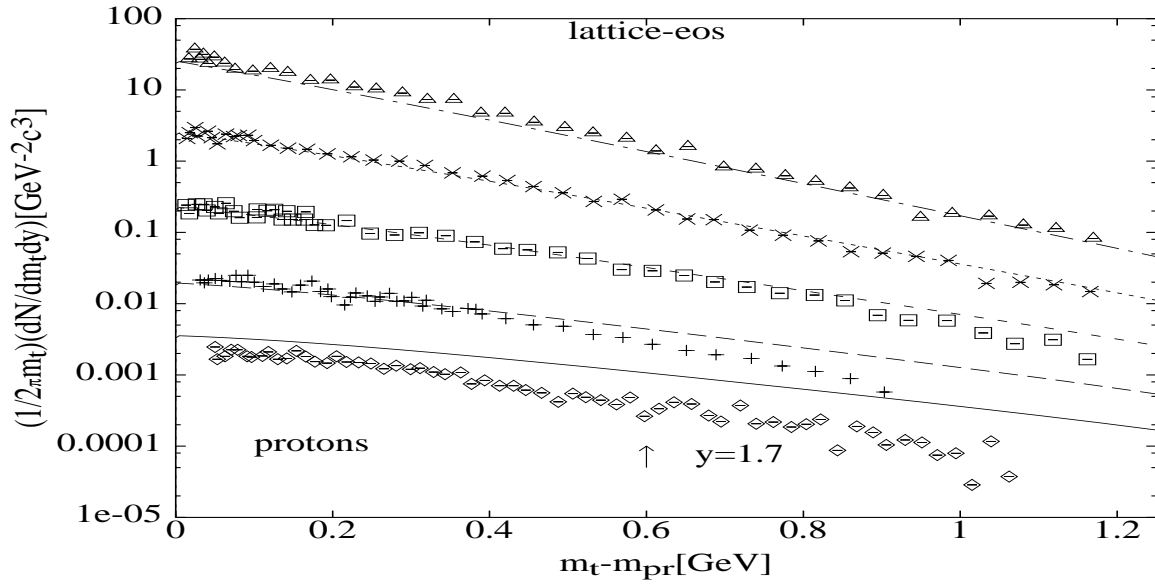
FIGURE 4
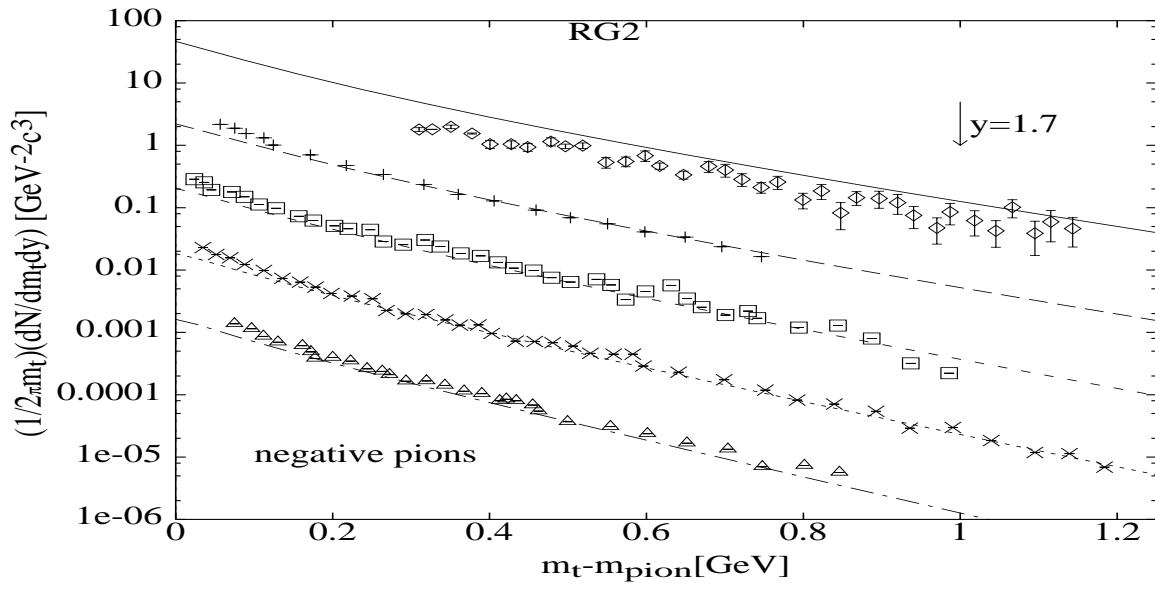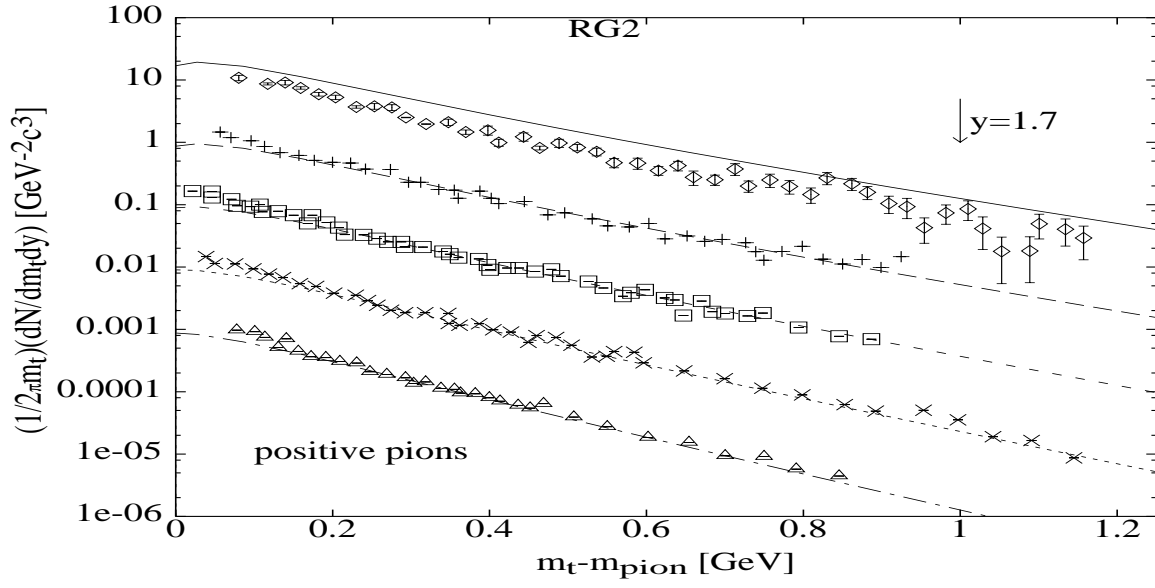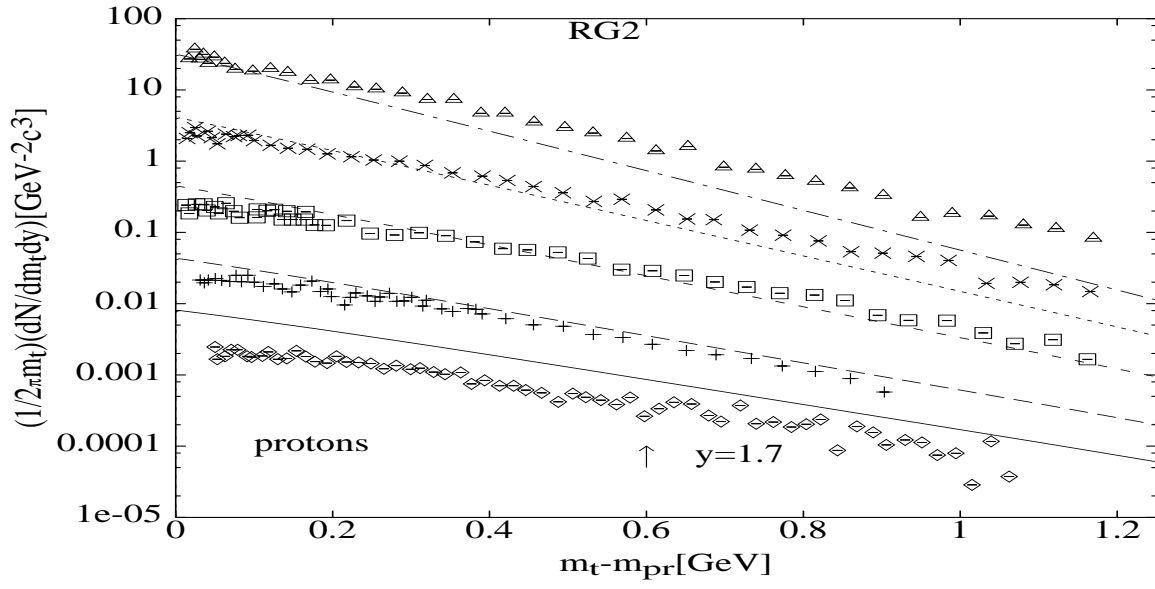
FIGURE 5
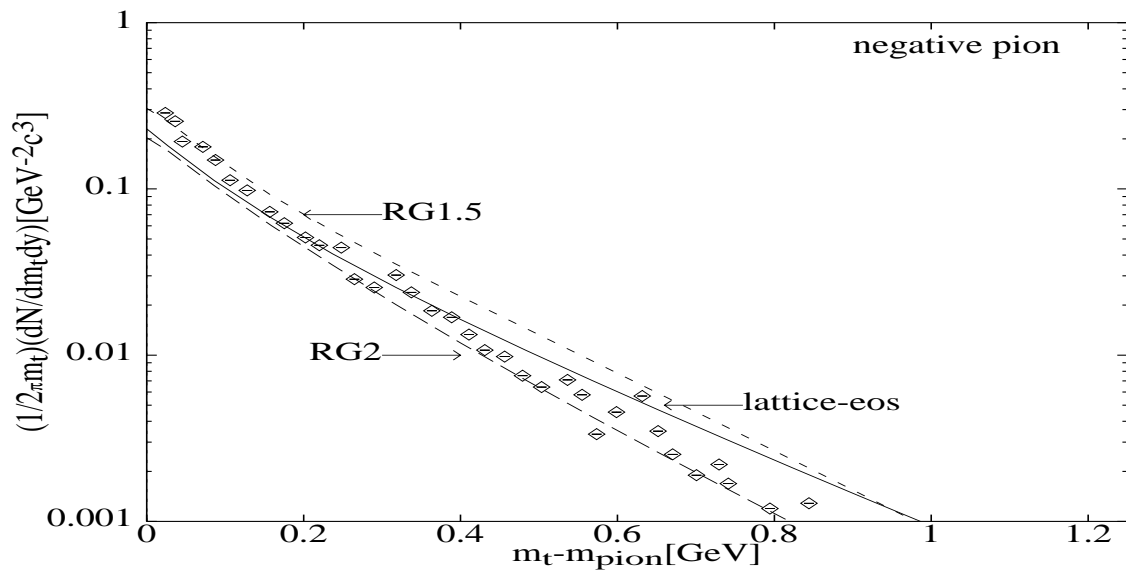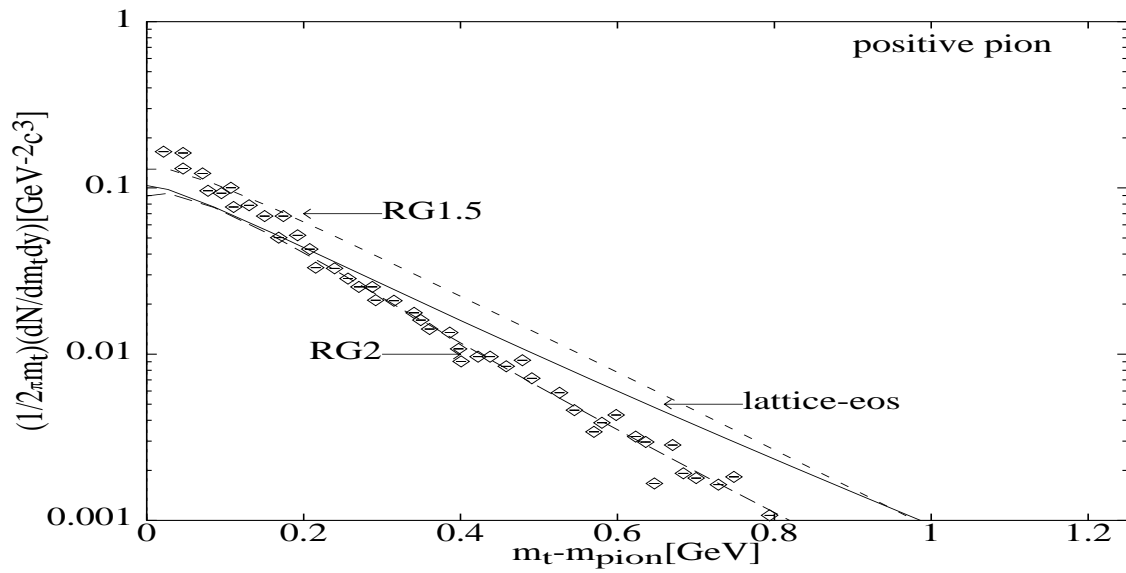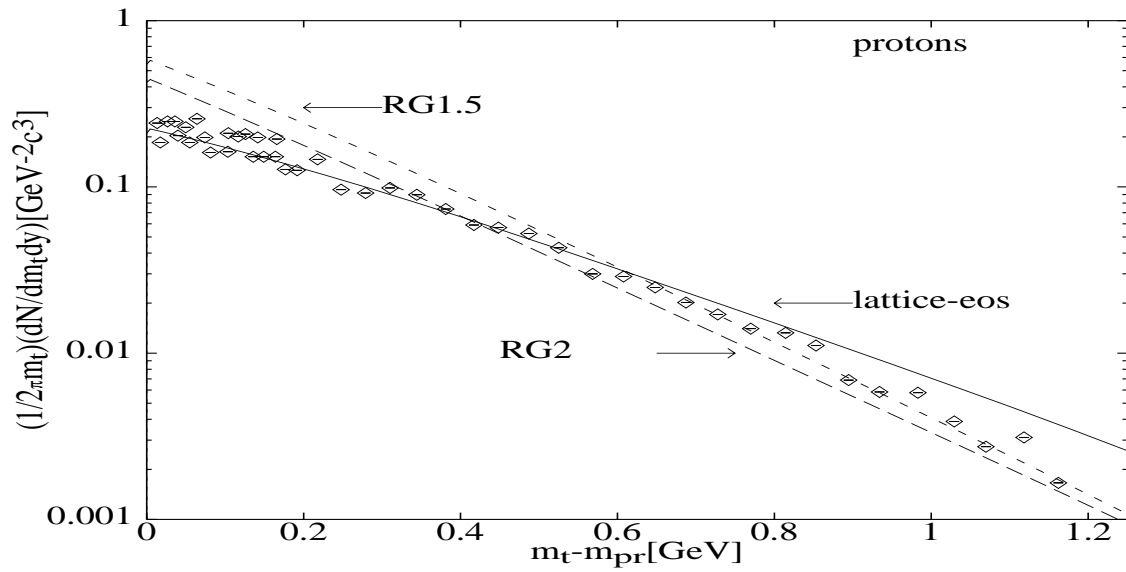
FIGURE 6
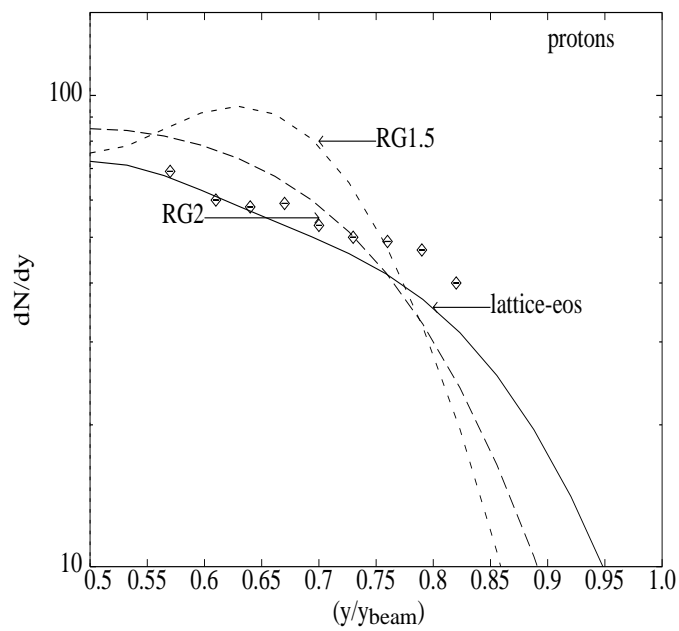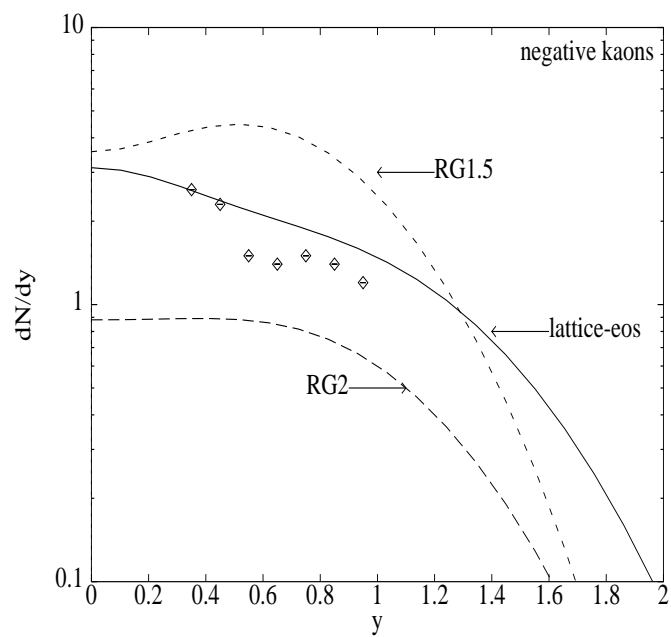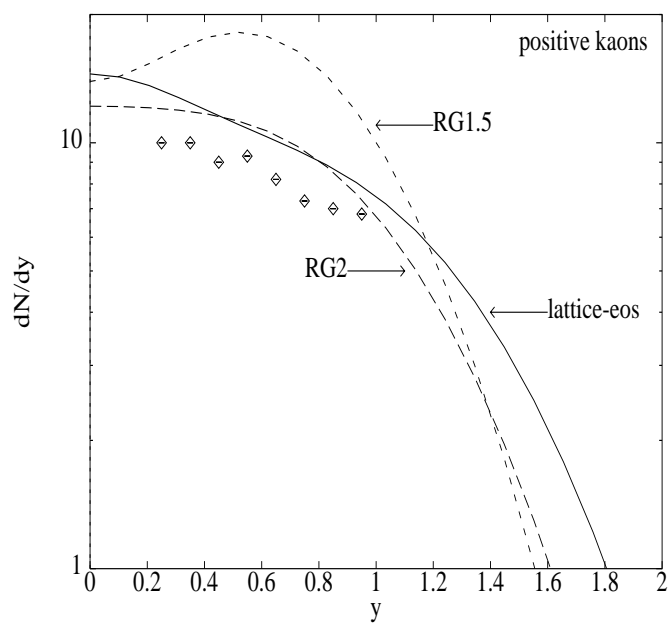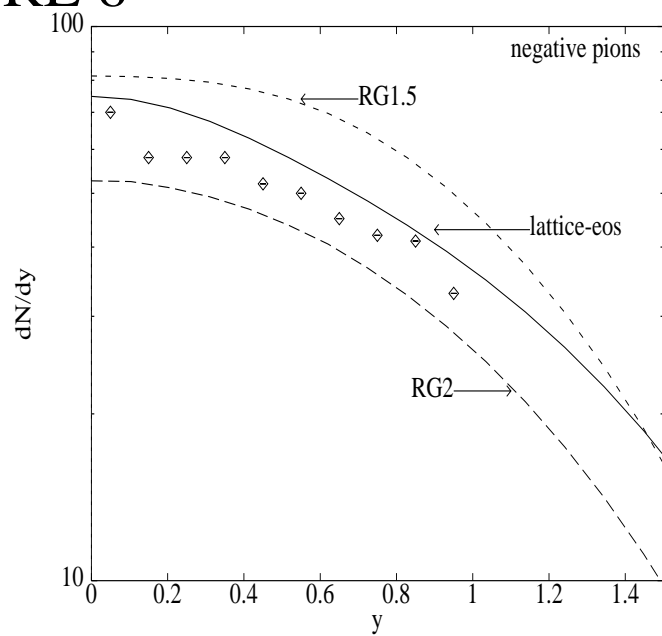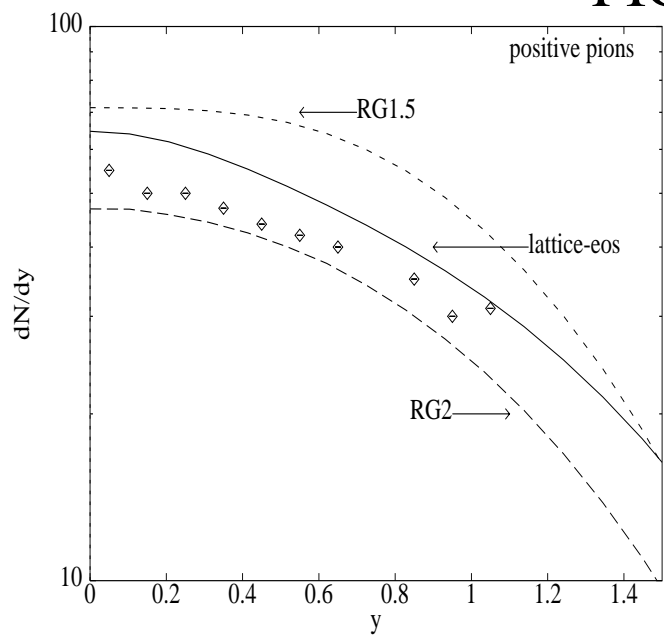
FIGURE 7

FIGURE 8

FIGURE 9